Epilepsia, 52(12):2344–2355, 2011
doi: 10.1111/j.1528-1167.2011.03312.x

FULL-LENGTH ORIGINAL RESEARCH

Spatiotemporal organization and thalamic modulation of seizures in the mouse medial thalamic-anterior cingulate slice

***Wei-Pang Chang, †Jiun-Shian Wu, ‡Chia-Ming Lee, §Brent A. Vogt, and *‡Bai-Chuang Shyu**

***Graduate Institute of Life Sciences, National Defense Medical Center, Taipei, Taiwan; †Institute of Zoology, National Taiwan University, Taipei, Taiwan; ‡Institute of Biomedical Sciences, Academia Sinica, Taipei, Taiwan; and §Cingulum NeuroSciences Institute, Manlius, New York, U.S.A.**

Summary

Purpose: Seizure-like activities generated in anterior cingulate cortex (ACC) are usually classified as simple partial and are associated with changes in autonomic function, motivation, and thought. Previous studies have shown that thalamic inputs can modulate ACC seizure, but the exact mechanisms have not been studied thoroughly. Therefore, we investigated the role of thalamic inputs in modulating ACC seizure-like activities. In addition, seizure onset and propagation are difficult to determine in vivo in ACC. We studied the spatiotemporal changes in epileptiform activity in this cortex in a thalamic–ACC slice to clearly determine seizure onset.

Methods: We used multielectrode array (MEA) recording and calcium imaging to investigate the modulatory effect of thalamic inputs in a thalamic–ACC slice preparation.

Key Findings: Seizure-like activities induced with 4-aminopyridine (4-AP; 250 μM) and bicuculline (5–50 μM) in ACC were attenuated by glutamate receptor antagonists, and the degree of disinhibition varied with the dose of bicuculline. Seizure-like activities were decreased with 1 Hz thalamic stimulation, whereas corpus callosum stimulation could increase ictal discharges. Amplitude and duration of cingulate seizure-like activities were augmented after removing thalamic inputs, and this effect was not observed with those induced with elevated bicuculline (50 μM). Seizure-like activities were initiated in layers II/III and, after thalamic lesions, they occurred mainly in layers V/VI. Two-dimensional current-source density analyses revealed sink signals more frequently in layers V/VI after thalamic lesions, indicating that these layers produce larger excitatory synchronization. Calcium transients were synchronized after thalamic lesions suggesting that ACC seizure-like activities are subjected to desynchronizing modulation by thalamic inputs. Therefore, ACC seizure-like activities are subject to desynchronizing modulation from medial thalamic inputs to deep layer pyramidal neurons.

Significance: Cingulate seizure-like activities were modulated significantly by thalamic inputs. Repeated stimulation of the thalamus efficiently inhibited epileptiform activity, demonstrating that the desynchronization was pathway-specific. The clinical implications of deep thalamic stimulation in the modulation of cingulate epileptic activity require further investigation.

KEY WORDS: Cingulate cortex, Thalamocortical system, Limbic seizures, Epilepsy.

Although frontal lobe epilepsy is one of the most prevalent types of seizure (McCagh et al., 2009), it receives less attention because clinical electroencephalography (EEG) can be normal in status epilepticus (Rasmussen, 1983; Shulman, 2000). Seizure discharges can originate in different zones of the frontal lobes, and among these seizure-prone zones, the anterior cingulate cortex (ACC) is one of the most difficult to identify with regard to onset (Mazars, 1970; Geier et al., 1977; Nadkarni & Devinsky, 2009). Patients with ACC epilepsy often show motor and autonomic symptoms and alterations in consciousness. Other symptoms, such as emotional outbursts, sudden fear, and rage, are also common (Chauvel et al., 1992; Devinsky et al., 1995; Nadkarni & Devinsky, 2009). These clinical symptoms have been described as part of the epileptic syndrome of frontal origin, which is the hallmark of seizures affecting area 24 (Bancaud & Talairach, 1992). Despite clinical evidence demonstrating that ACC is involved in partial epileptic disorders, the mechanism of seizure onset, spatiotemporal propagation, and synchronization in this region are not well understood.

Thalamic afferents may regulate ACC seizure discharges. The ACC is heavily connected with the midline, mediodorsal, and intralaminar thalamic nuclei (MITN) (Vogt et al., 1987; Hatanaka et al., 2003; Vogt, 2005), and the medial thalamus (MT) could play a pivotal role in the remote

Accepted September 16, 2011; Early View publication November 16, 2011.

Address correspondence to Bai-Chuang Shyu, 128 Academia Road, Section 2, Nankang, 11529, Academia Sinica, Taipei, Taiwan. E-mail: bmbai@gate.sinica.edu.tw

control of seizure synchronization (Kahane & Depaulis, 2010). Studies of generation mechanisms of spike-wave discharges (SWDs) using the genetic Absence Epilepsy Rat from Strasbourg showed that SWDs can be generated endogenously within somatosensory cortex (Polack et al., 2009). When thalamic activity was blocked by tetrodotoxin (TTX), epileptiform cortical activity resulted in a longer sequence of SWDs, indicating that thalamic inputs might modulate it. Prolongation of epileptiform activities could be caused by desynchronization following tonic firing in ventral-medial thalamocortical neurons (Glenn et al., 1982). Previous studies have also shown that noxious stimulation can increase medial thalamic activities and desynchronize cortical EEG (Antognini et al., 2000). Whether the desynchronizing effect of thalamic inputs can block seizures has not been studied. Therefore, our hypothesis was that the ACC is responsible for seizure generation and that inputs from the MT might alter the synchronization of epileptiform activities.

The convulsant 4-aminopyridine (4-AP) induces epileptic discharges in humans (Lundh et al., 1984) and other mammals (Glover, 1982). Many in vitro studies show that 4-AP induces epileptiform activities in parahippocampal cortex (Avoli et al., 1996), cingulate cortex (Panuccio et al., 2009), and the amygdala (Klueva et al., 2003). 4-AP–induced seizure-like activities are sensitive to anticonvulsants, and pharmacoresistant activities can be induced by combining the γ-aminobutyric acid $(GABA)_A$ antagonist bicuculline with 4-AP (Bruckner et al., 1999). Therefore, in the present study we used 4-AP and various doses of bicuculline to induce seizure-like activities in ACC to study pharmacoresistant seizures. Although epileptiform activity in rat cingulate cortex has been characterized in coronal slices (Panuccio et al., 2009), long-distance fibers were severed during slice preparation. The present study used a thalamocingulate slice preparation (Lee et al., 2007) to investigate the spatiotemporal changes in epileptiform activity in the cingulate cortex and the involvement of inputs from the medial thalamus (MT) in modulating ACC seizures.

Materials and Methods

Animals

Male C57BL/6J mice (4 weeks old) were used, and all research conformed to National Institutes of Health (NIH) guidelines in accordance with the Institutional Animal Care and Utilization Committee, Academia Sinica (Taipei, Taiwan). Every effort was made to minimize the number of animals used.

Slice preparation

Animals were anesthetized (4% halothane in pure oxygen), and the brains were quickly removed and cooled for 3 min in chilled, oxygenated artificial cerebrospinal fluid (aCSF) (124 mM NaCl, 4.4 mM KCl, 1 mM NaH_2PO_3, 2 mM $MgSO_4$, 2 mM $CaCl_2$, 25 mM $NaHCO_3$, and 10 mM glucose, bubbled with 95% O_2 and 5% CO_2). The slice containing the thalamocingulate pathway was prepared according to the method established previously (Lee et al., 2007). All slices were incubated in oxygenated aCSF at room temperature for 1 h. A single slice was then transferred to the recording chamber and kept at 29–30°C under continuous perfusion (12 ml/min) of oxygenated aCSF.

Extracellular recording

Multielectrode arrays (MEAs) were used to record the spatiotemporal properties of epileptiform activity. Two types of MEAs were used: 6×10 planar MEA (electrode diameter, 30 μm; electrode spacing, 500 μm; impedance, 50 kΩ at 200 Hz; Multi Channel Systems, Reutlingen, Germany) and 8×8 MEA (pyramidal-shaped electrode diameter, 40 μm; tip height, 50 μm; electrode spacing, 200 μm; impedance, 1,000 kΩ at 200 Hz; Ayanda Biosystem, Lausanne, Switzerland). Data were acquired using MC Rack software (Multi Channel Systems) at a 10 kHz sampling rate.

Corecording calcium images and MEA

Slices were placed on the porous membrane (pore size, 0.4 μm) of a Millicell-CM culture transwell. Both the inside and outside of the transwell were filled with aCSF. The entire dish was kept in a moist environment with oxygen. A dye solution (3 μl) was then dropped on the surface of the slice. The dye solution was prepared with 48 μl dimethyl sulfoxide (DMSO; Sigma, St. Louis, MO, U.S.A.) and 2 μl F127 (10% in DMSO; Invitrogen, Carlsbad, CA, U.S.A.) in 50 μg Fluo4-AM (Invitrogen). Slices were incubated in the dark at 37°C for 30 min (Ikegaya et al., 2005). Slices were then transferred to the MEA probe chamber. The tissue was illuminated with a 488 nm laser (Coherent, Santa Clara, CA, U.S.A.) and images were acquired at 2–5 Hz using an upright LSM510 META microscope (Zeiss, Oberkochen, Germany) equipped with a water immersion lens (63× magnification, 1.1 N.A; 20× magnification, 0.7 N.A) or a fluorescence stereomicroscope (Zeiss). The fluorescence change over time was defined as $\Delta F/F = (F - F_{basal})/F_{basal}$, in which F was the fluorescence at any time point, and F_{basal} was the baseline fluorescence averaged across the entire image for each cell. The correlations between calcium transients recorded in different cells were assessed by cross-correlation analysis.

Data analysis

Data were analyzed by MC Rack software (Multi Channel Systems) and the subroutines for the MATLAB program (MathWorks, Natick, MA, U.S.A.). To detect oscillatory events, we set three standard deviations (SD) of the noise level as the threshold. The amplitudes of the peaks during an oscillation event that surpassed this threshold were automatically detected by MC RACK software. The time point

of each peak that exceeded this threshold was also detected, and the duration of an oscillation event was measured by subtracting the time point between the first and last peaks that surpassed the threshold. Two-dimensional (2D) current-source density (CSD) profiles were calculated from the field potential profiles (Shimono et al., 2001). To cover all cortical area, 8 × 8 MEA with 200 μm electrode spacing was used in the experiment. Local field potentials were low-pass filtered at 100 Hz, and data were spatially smoothed by 3 × 3- weighted average kernel. The results were convolved with a 3 × 3 Laplacian kernel to produce a discrete approximation of the second spatial derivative. Current-versus-time plots for single points in the slice were obtained by computing the 8 × 8 CSD for each time step and calculating the value at the desired location via bilinear interpolation. The field potential values of some recording electrodes were obtained by interpolating averaged responses from neighboring electrodes. CSD data on boundary sites were obtained by extrapolation. Color image plots were generated to facilitate visualization of CSD profiles. Blue represents current sinks and red represents current sources.

Data in the text are expressed as mean ± standard error (SE). Statistical analyses were performed with Systat (SPSS, Chicago, IL, U.S.A.) and Microsoft Excel using Student's *t*-test. Measurements in the text are expressed as mean ± SE, and n indicates the number of slices or neurons studied. The results were considered significant when $p \leq 0.05$.

Results

Properties of 4-AP/bicuculline-induced oscillations

Multichannel epileptiform activities induced by 4-AP (250 μM) and bicuculline (5 μM) were recorded by MEAs and superimposed on a contour depicting a relative recording position on an MT–ACC slice (Fig. 1A). Typical traces were selected for magnification in Fig. 1B. Typical 4-AP (250 μM) + bicuculline-induced seizure-like activities were composed of an ictal onset (Fig. 1B, arrow), followed by a tonic phase (Fig. 1B, red line) and long-duration high-frequency population bursts of (8.1 Hz) clonic phase (Fig. 1B, green line). The duration of the clonic phase (Fig. 1B, green line) was decreased significantly after application of 2R-amino-5-phosphonovaleric acid (APV) (50 μM; Fig. 1B, middle panel). Further application of 6-cyano-7-nitroguinoxaline-2,3-dione (CNQX) (20 μM) completely abolished the clonic phase and decreased the amplitude and duration of ictal onset (Fig. 1B, arrows, lower panel). The statistical results showed that the duration and amplitude of oscillations were decreased significantly after application of APV and CNQX (n = 12, *p < 0.05, *t*-test; Fig. 1D). Therefore, 4-AP/bicuculline-induced seizure-like activities in the MT–ACC slice are susceptible to glutamate receptor antagonists, and excitatory amino acids are involved in the clonic phase.

Application of muscimol (1 or 3 μM) to the slices significantly reduced the amplitude and duration of oscillatory activity. A higher concentration of muscimol (5 μM) completely blocked the response (Fig. 1C); the effects of muscimol on the amplitude and duration of epileptiform activity are shown in Fig. 1D (n = 7, *p < 0.05, *t*-test). To demonstrate that 5 μM bicuculline only partially blocked GABAergic transmission, the dose of bicuculline was increased to 50 μM. At 50 μM bicuculline, 5 or 50 μM muscimol did not suppress epileptiform activity, which demonstrated that 50 μM bicuculline fully blocks GABAergic transmission.

Modulation of epileptiform activity with MT and corpus callosum electrical stimulation

Connectivity between thalamus and cortex was tested in all experiments. Prior to each experiment, each slice was checked for the integrity of the MT–ACC pathway. Only those slices with local field potentials in ACC evoked by delivering small amount of currents in MT were used in experiment. The MT- and corpus callosum (CC)–evoked cingulate responses are shown in Fig. 2A, including positions of the stimulation and recording electrodes. Electrical stimulation of each site in the presence of 4-AP/bicuculline evoked epileptiform activities as an all-or-none event because the amplitude and duration of oscillation were not influenced by changing the intensities of the electrical stimuli ≥50 μA (Fig. 2B). The stimulation intensity was tested and adjusted to threefold the threshold sufficient to induce oscillation (150 μA). The duration and amplitude of the oscillation evoked by CC stimulation were significantly larger than the MT stimulation (n = 15, *p < 0.05, *t*-test; Fig. 2C). The firing pattern induced by electrical stimulation in the MT or CC was compared using intracellular recording (see Fig. S1). The duration and peak firing frequency were higher in the CC stimulation groups (n = 5, *p < 0.05, *t*-test).

Cortical seizure-like activities induced by 4-AP/bicuculline could be modulated by different stimulation frequencies in the MT and CC. In the presence of 4-AP and bicuculline, single-shock stimulation of the MT with a 0.1 Hz frequency induced ACC oscillation (Fig. 2D, upper trace). However, a further increase in the stimulation frequency from 0.5 to 1 Hz reduced the occurrence of seizure-like activities (Fig. 2D, middle and lower traces). One Hertz stimulation in the MT suppressed the seizure-like activities (n = 8, *p < 0.05, *t*-test). Stimulation with 1 Hz in the CC also lowered the percentage of induced epileptiform activity, but this was less effective than thalamic stimulation (n = 5, *p < 0.05, *t*-test; Fig. 2E,F, left panel). Medial thalamic stimulation–inhibited epileptiform activity was reflected by a prolonged interval of occurrence compared with spontaneous seizure-like activities (n = 9, *p < 0.05, *t*-test; Fig. 2F, right panel). CC stimulation significantly reduced the interevent interval of seizure-like

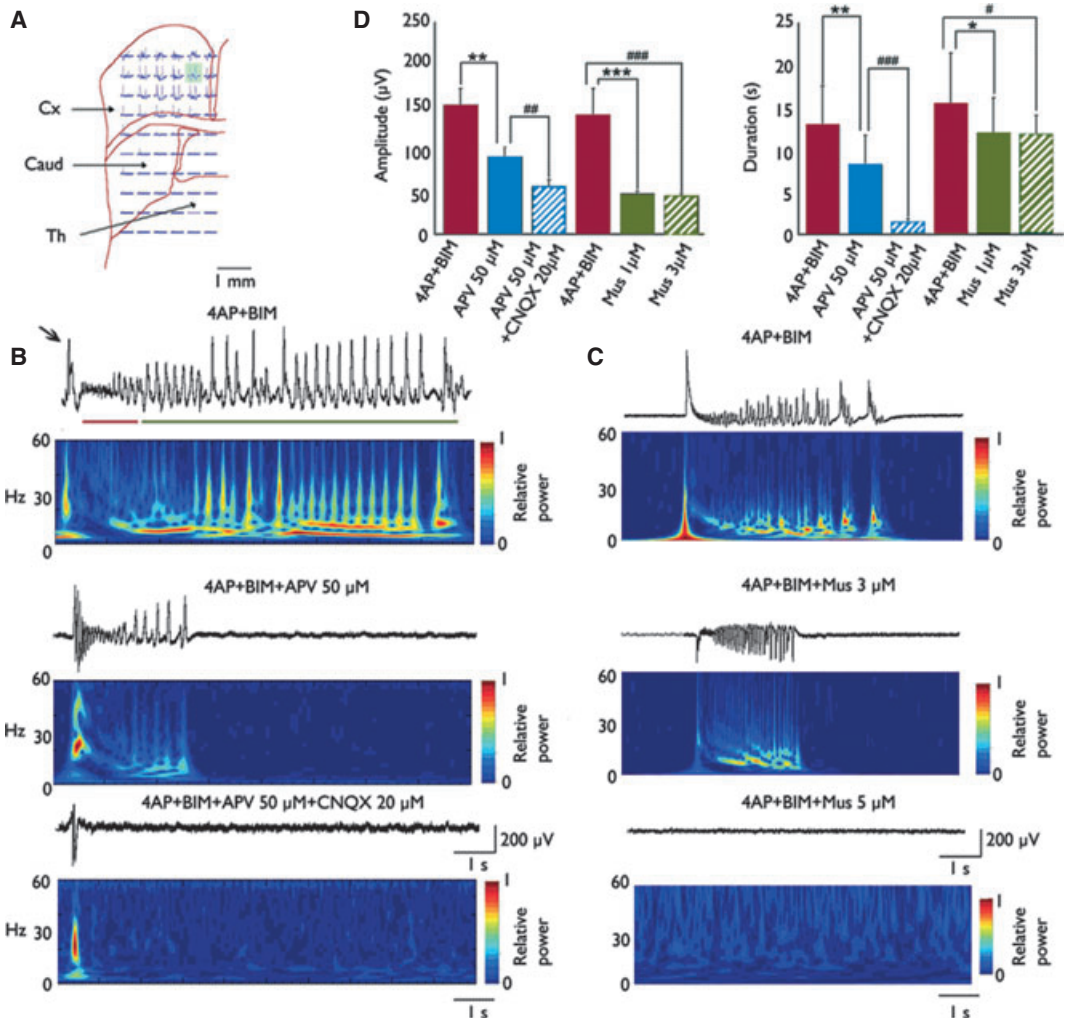

Figure 1.

Pharmacologic characterization of 4-AP/bicuculline-induced epileptiform activity in the MT-ACC slice. (**A**) Relative positions of the electrodes in the MT-ACC slice and ensemble of epileptiform activity. (**B**) The green square–encircled channel was selected for magnification to show a typical trace of epileptiform activity induced by 4-AP (250 μM) and bicuculline (5 μM). Epileptiform activity consisted of an ictal onset followed by tonic (red line) and clonic (green line) discharges. After application of APV (50 μM), a significant decrease in clonic phase was observed. Subsequent application of CNQX (20 μM) further abolished clonic phase. Only ictal onset remained, although with a smaller amplitude and duration. (**C**) Typical 4-AP (250 μM)/bicuculline (5 μM)-induced epileptiform activity in another experiment. Application of muscimol (3 μM) attenuated and reversed the polarity of epileptiform activity and a higher dose of muscimol (5 μM) completely blocked the response. (**D**) The amplitude and durations were decreased significantly after application of the glutamate antagonists APV and CNQX. A low dose of the GABA agonist muscimol significantly inhibited epileptiform activity. Caud, caudate; Cx, cortex; Th, thalamus.

activities (n = 5, *p < 0.05, *t*-test; Fig. 2F). Therefore, the suppressive effect was pathway-specific, and thalamic inputs may play a dominant role.

Thalamic inputs inhibit the initiation and progression of oscillations

MEA recording was used to define the site of initial bursts and modulation of this initial activity by MT inputs. Typical burst activity is shown in Fig. 3A-a. The channel that first reached 3 SD of the noise level was denoted as the initial point. MEA was used to identify the initiation onset of each epileptiform discharge. The distribution of initial onsets obtained from intact and thalamic denervated groups are displayed in Fig. 3A-b. When thalamic inputs were intact, seizure-like activities preferentially began in layers II/III and V. However, after the thalamic inputs were removed, the initiation site shifted to layers V/VI (Fig. 3A-c). Superimpositions of 2D CSD analysis of ictal onsets (n = 7)

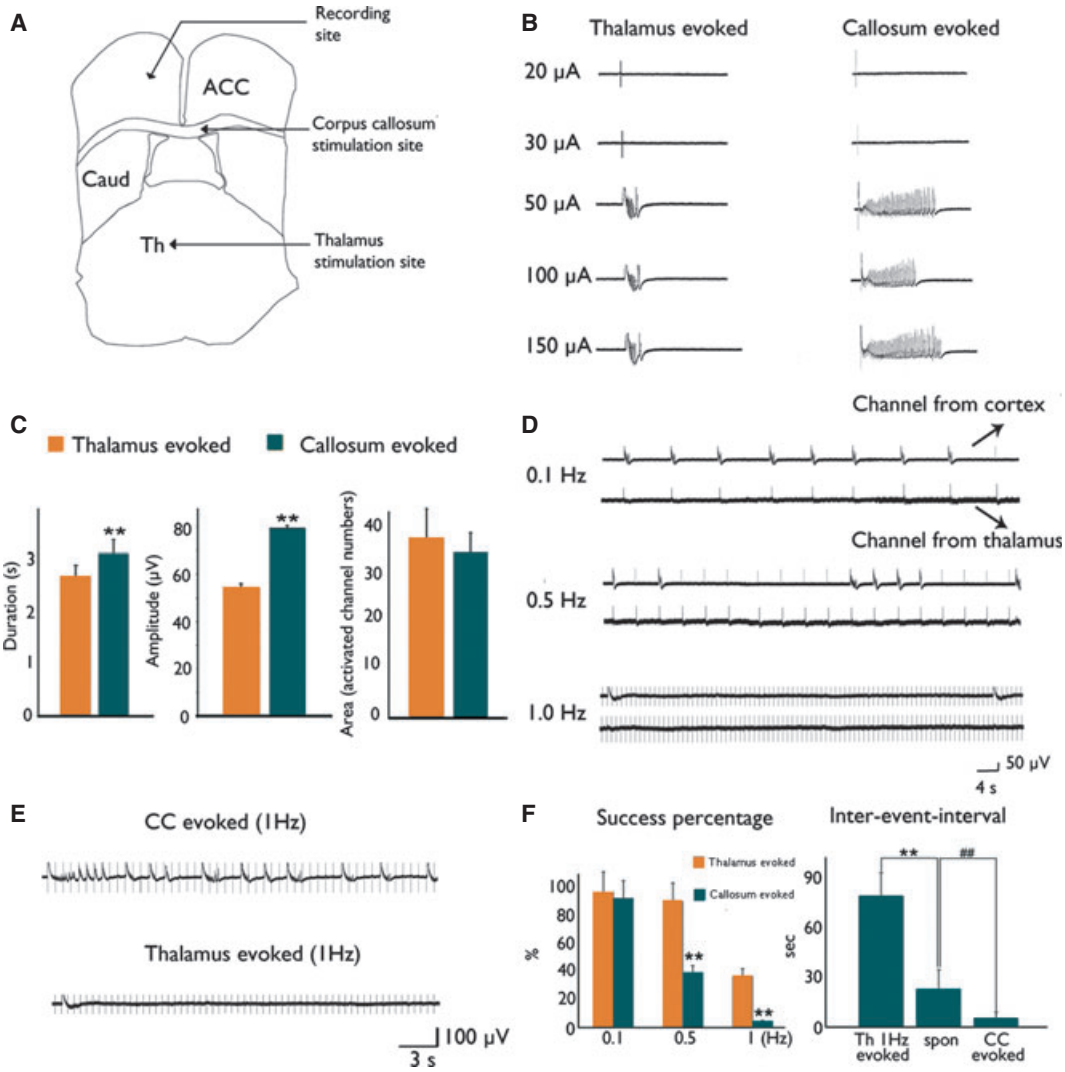

Figure 2.

Simulation in the MT suppressed epileptiform activity induced by 4-AP/bicuculline in ACC. (**A**) The stimulation sites in the MT and CC and recording site in ACC. (**B**) Activity following MT and CC stimulation were all-or-none. Oscillations were not altered in response to various stimulation intensities within each group, but the duration and amplitude of the oscillation elicited by direct cortical stimulation was higher than thalamic stimulation. (**C**) The duration and amplitude of epileptiform activity generated with 4-AP were significantly greater in response to CC stimulation than that for MT stimulation. The areas involved in oscillation as calculated by summing the activated recording channels were not significantly different between the two groups. (**D**) Stimulation in the MT with 0.1 Hz evoked ACC epileptiform activity in all cases. Stimulation with 0.5 Hz was only evoked in half of the cases. Epileptiform activity was seldom evoked with 1 Hz stimulation. (**E**) In comparison of 1 Hz stimulation in the CC and MT, CC stimulation induced more oscillation than thalamus stimulation alone in the presence of 4-AP and bicuculline. (**F**) The left panel shows the statistical results, indicating that with 0.1 Hz stimulation, almost every stimulation evoked ACC epileptiform activity by both the MT and CC stimulation, whereas with 0.5 Hz stimulation, only 41.2% stimulation in the MT evoked cortical epileptiform activity. Stimulation with 1 Hz stimulation evoked seizure-like activities in only a few cases, which was significantly lower compared with CC stimulation. The right panel shows the statistical results of the interevent interval during 1 Hz MT and CC stimulation-induced epileptiform activity and spontaneous epileptiform activity. Thalamic stimulation with 1 Hz significantly prolonged the interval compared with spontaneously occurring epileptiform activity. Caud, caudate; CC, corpus callosum; Cx, cortex; Th, thalamus.

indicated that when the thalamic inputs were intact, the source currents (red) aggregated in layer V while sink current (blue) occurred more frequently in superficial layer. When the thalamic inputs were removed, the source currents shifted to superficial layers and sink current occurred more frequently in layers V/VI (Fig. 3A-d). Therefore, thalamic inputs exert a modulatory effect on the initiation of the cingulate seizure-like activities in deep layers.

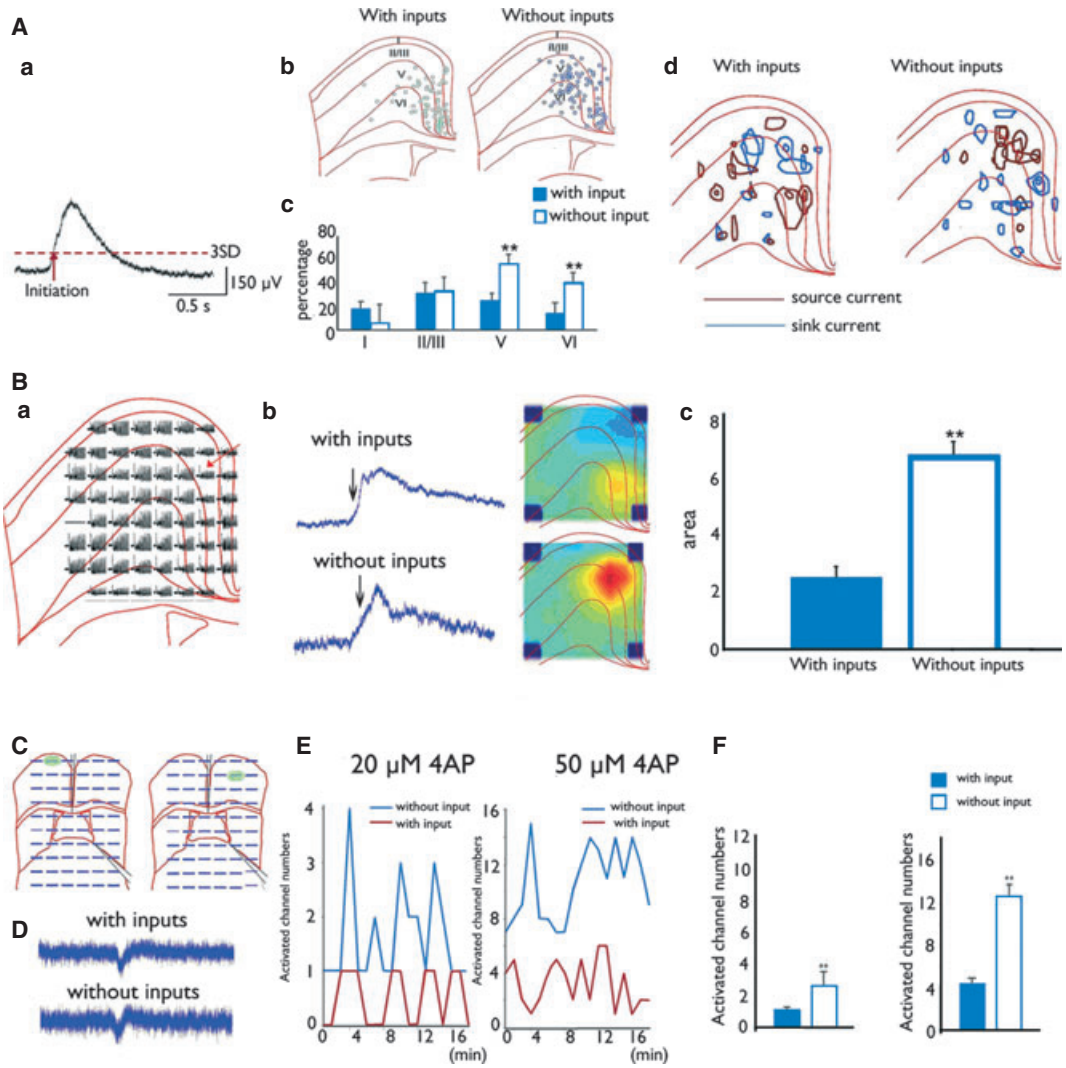

Figure 3.
ACC lacking MT inputs is more susceptible to initiation of seizure-like activities. (**A**) (**a**) Red dashed line indicates the three SD of the noise level. The channel in which activity was first surpassed was used as the threshold (arrows) of initiation. (**b**) Distribution of initiation point in the two groups. (**c**) Distribution of initiation points in different layers. (**d**) Sink signals occurred more in deep layer after thalamic inputs were removed compare to control group. (**B**) (**a**) Ensemble epileptiform activities; a typical channel was selected for magnification in **b**. (**b**) Isopotential color map of the time point (arrows indicated in the traces). Notice that ACC with severed thalamic inputs are associated with larger areas. (**c**) In the group with severed thalamic inputs, larger areas were involved in the initiation of epileptiform activity. (**C**) Orientation of slice with respect to electrodes and cutting position. (**D**) Enlarged response of low-dose 4-AP (20 μM)-induced activity. (**E**) Time-lapse experiment showing that more activated channels were evident in the group without thalamic inputs at all time points. This result was also significant when the concentration of 4-AP was 50 μM. (**F**) Seizure-like activities were more readily evoked in the thalamic lesion group to low-dose 4-AP (20 or 50 μM).

Thalamic inputs influenced spreading areas of seizure-like activities. Typical ensemble activity in Fig. 3B showed that seizure-like activities were engaged in most cortex (arrow indicates channel for subsequent analysis). The seizure-prone areas were compared when the activity reached a half maximum of the amplitude of ictal onset (Fig. 3B-b) and areas involved in epileptiform activities were significantly larger when the thalamic inputs were removed ($n = 6$, $^*p < 0.05$, *t*-test; Fig. 3B-c). Therefore, thalamic inputs exert a desynchronizing effect on the spread of ictal onsets.

Cortex lacking thalamic inputs is more susceptible to seizures

To determine whether cortex lacking thalamic inputs is more susceptible to seizures, the sensitivity of each side of

the slice was compared for generation of seizure-like activities. A low dose of 4-AP (20 μM) was used to induce ictal onsets and to avoid widespread seizure-like activities. The CC was incised to cut communication between hemispheres, and the right side of MT inputs was cut. Seizure-like activities were induced in ACC during low-dose 4-AP on both sides and seizure-like activities did not propagate from small areas (Fig. 3C, green circle; typical examples in Fig. 3D). Therefore, the cortex itself is sufficient to generate epileptiform activity and regions lacking thalamic inputs are more prone to generation of seizure-like activities. A low dose of 4-AP (20 μM), showed that the side that did not have thalamic inputs was more prone to epileptiform activity ($n = 7$, $^*p < 0.05$, *t*-test; Fig. 3E,F, left panel). Increasing the dose of 4-AP to 50 μM showed that epileptiform activity increased in both the side with intact thalamic inputs and the side that lacked them. Epileptiform activity also occurred more in the side that lacked thalamic inputs ($n = 7$, $^*p < 0.05$, *t*-test; Fig. 3E,F, right panel). Therefore, ACC that lacks thalamic inputs is more susceptible to the generation of seizure-like activities.

Tonic thalamic inputs block long-lasting oscillations in deep layers

To elucidate the relative contribution of tonic thalamic inputs in the modulation of cingulate seizures, we compared seizure-like activities without the influence of MT inputs. Because seizure-like activities are synchronized between the right and left cortices, the CC was incised to sever communication between hemispheres such that unilateral MT lesion effects can be isolated. An incision was made in the right pathway between the MT and ACC during brain slicing (Fig. 4A), whereas the left MT-ACC pathway remained intact. No significant difference in the amplitude and duration of epileptiform activity was observed between the left and right cortices after cutting the CC.

Seizure-like activities generated with 4-AP (250 μM)/bicuculline (5 μM), which arose from the intact MT side (left side), were initiated in the ACC and propagated to the thalamus (Fig. 4B, upper panel). Activity arising from the side without MT inputs (right side) was restricted to the cortex and did not propagate to thalamus (Fig. 4B, lower panel) because the connections between MT and ACC were severed. Activity arose from both sides and a typical example is shown in Fig. 4C. The amplitude and duration were significantly smaller in the cortex with intact thalamic inputs ($n = 10$, $^*p < 0.05$, *t*-test; Fig. 4D). Local application of lidocaine in medial thalamus also significantly enhances the durations of seizure-like activities in cingulate cortex ($n = 6$) (see Fig. S2).

When increasing the concentration of bicuculline to 50 μM and presumably completely blocking GABAergic transmission, the significant differences in the amplitudes and durations of oscillations disappeared ($n = 9$, $^*p < 0.05$, *t*-test; Fig. 4D). Therefore, GABAergic transmission plays an important role in the thalamic desynchronization of cingulate oscillations.

The changes in the spatiotemporal properties of epileptiform activity in response to MT incision are illustrated by field potential recording. The response were normalized to maximal value and divided into three groups: >50% maximal response (red dots), 25–50% (green dots), and <25% (black dots; Fig. 4E). When the MT inputs were removed, seizure-like activities exhibited significant alterations in amplitude and duration. The average amplitude of seizure-like activities increased significantly from 191.2 ± 13.3 μV in the intact thalamic input group to 243.3 ± 19.6 μV in the severed thalamic input group in layer V ($p < 0.05$), and there was a significant difference between the two groups in layer V (Fig. 4F, left panel). Duration also changed significantly from 7.5 ± 1.9 to 10.6 ± 2.6 s in layer V and 6.9 ± 1.4 to 9.6 ± 2.5 s in layer VI without thalamic inputs (Fig. 4F, right panel). Seizure-like activities recorded in layers II/III also had a longer duration compared with lateral cortex (Fig. 4E). Therefore, removal of thalamic inputs shifted epileptiform activity to the deeper layers (Fig. 4E,F). Removing MT inputs also significantly enhanced vertical propagation velocity ($n = 9$) (see Fig. S3).

Calcium imaging revealed that MT inputs desynchronize epileptiform activity

Previous studies indicated that calcium is involved in the generation of bursting activity during seizures (Contreras & Llinas, 2001; Traub et al., 2005). Therefore, calcium imaging was used to investigate the synchronization of neuronal population activity. Calcium activity induced by 4-AP/bicuculline was recorded with and without thalamic inputs (Fig. 5A) and calcium imaging and MEA recording were performed simultaneously. MEA demonstrated that most oscillatory activity was initiated at layers II/III and V, and calcium imaging was focused on these layers (green box in Fig. 5A) to study the synchronization between individual cells with and without thalamic inputs.

Calcium-wave oscillations were induced with 4-AP/bicuculline (Fig. 5B, upper panel), and the calcium oscillation of a neuron was correlated with the field potentials (Fig. 5B, middle panel, magnified in lower panel). The dynamic calcium images were compared in groups with and without MT input. All calcium-image traces from individual cells were aligned, and the average traces are shown. The average $\Delta F/F$ was 1.62 ± 0.23 from side with intact thalamic inputs and 1.03 ± 0.18 from side without thalamic inputs ($n = 6$, $^*p < 0.05$, *t*-test). The average peaks appeared significantly larger on the side with severed thalamic inputs ($n = 6$, $^*p < 0.05$, *t*-test; Fig. 5C). Calcium-image transients during bursting are also shown on a 3D plot. At this time point, the $\Delta F/F$ of the calcium image was significantly stronger in the severed thalamic input group compared with the intact group ($n = 6$, $^*p < 0.05$, *t*-test). Typical response

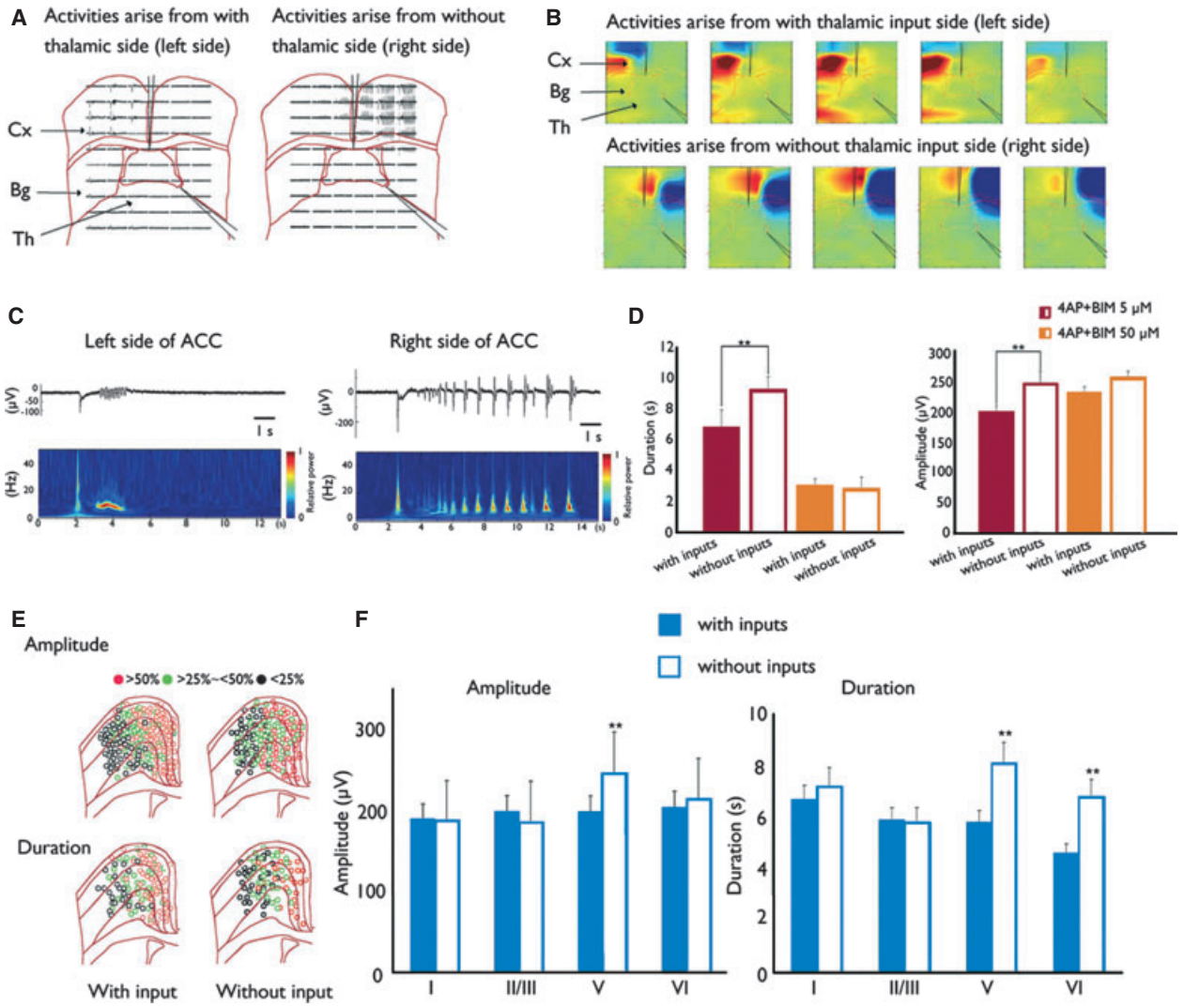

Figure 4.

Modulatory role of thalamic inputs during cortical seizure-like activities. (**A**) Cut positions, one in the middle of the corpus callosum and one at the border between the thalamus and basal ganglia in the right hemisphere. Activity arising in the group without thalamic inputs was larger. (**B**) Pseudocolor isopotential map indicating that epileptiform activity arising from the group with intact thalamic inputs was first initiated in the cortex and then propagated to the thalamus. Epileptiform activity in the group with severed thalamic inputs was restricted to cortex and the basal ganglia. (**C**) Typical traces showing that epileptiform activity was significantly smaller in the side with intact thalamic inputs. (**D**) Summary results showing that the amplitude and duration of epileptiform activity were significantly larger in the group with severed thalamic inputs with the application of 250 μM 4-AP/5 μM bicuculline. When the concentration of bicuculline was increased to 50 μM, no significant difference was observed between groups. (**E**) Amplitude and duration of epileptiform activity were normalized to the maximal value and displayed in color code in different regions (>50% maximal response, red dots; 25–50%, green dots and <25%, black dots). A stronger response was observed in the medial dorsal region of the cortex. (**F**) Summary results of the layer distribution of the amplitude and duration of epileptiform activity in the groups with and without thalamic inputs. Cuad, caudate; Cx, cortex; Th, thalamus.

comparison is shown in Fig. 5D. Cross-correlation of calcium fluorescence between different cells was used as a synchronization index. In the severed thalamic input side, the correlation coefficient was higher (n = 6, *p < 0.05, *t*-test; Fig. 5E). Therefore, thalamic inputs exert a desynchronizing effect during ACC seizures.

Discussion

The MT–ACC slice preparation enabled us to evaluate the role of thalamic inputs in modulating cingulate seizures in ways that cannot be accomplished in vivo. Removing the thalamic inputs significantly modulated epileptiform activity

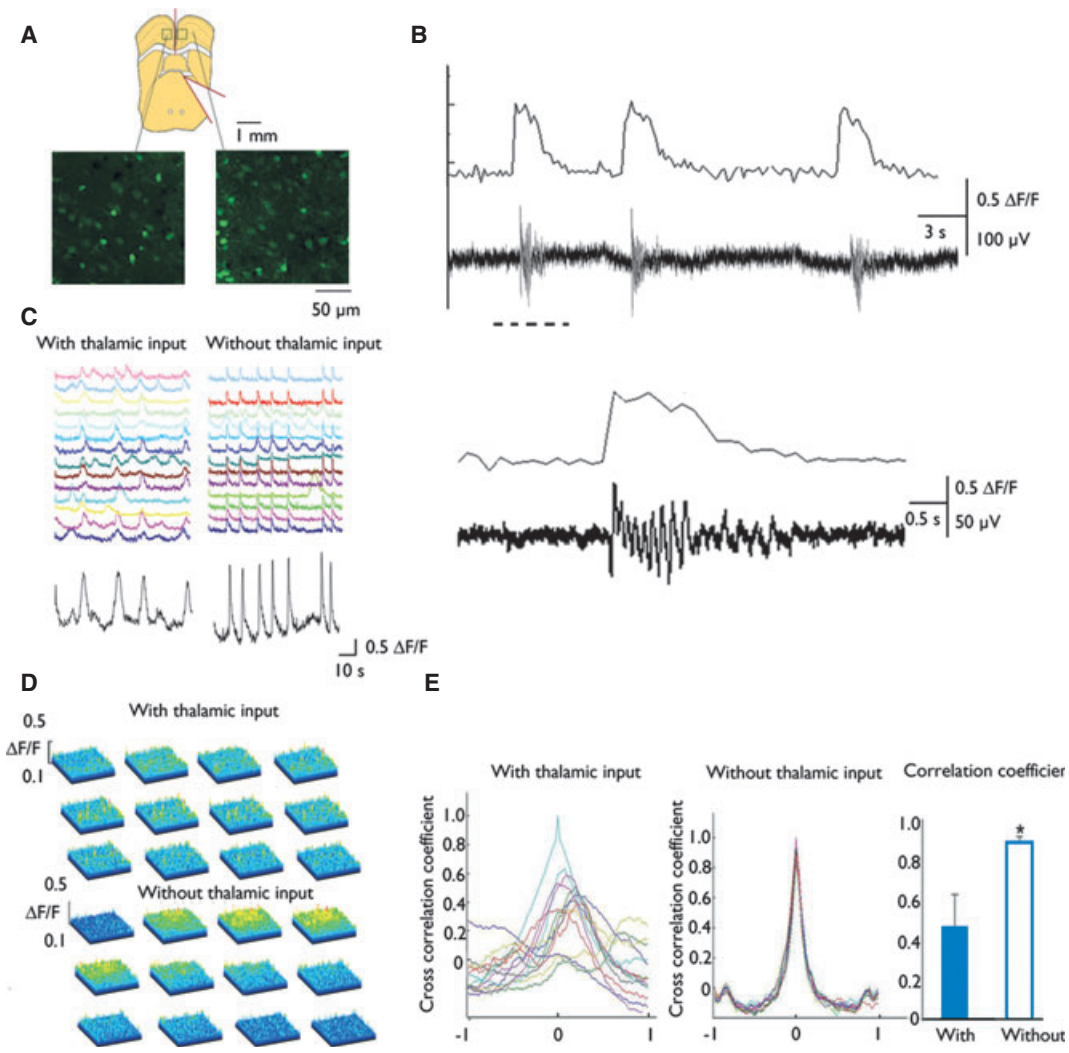

Figure 5.
Calcium imaging combined with MEA recording indicated that thalamic inputs desynchronize seizure-like activities. (**A**) Areas where calcium imaging was recorded in sides with and without thalamic inputs. (**B**) Calcium transients were corecorded with MEA activity. (**C**) Traces obtained from individual cells and the lower panel is the average. (**D**) Surface plot of entire view. The signal was processed as ΔF/F. Simultaneous recording of calcium signal and MEA recording. The calcium signal was corecorded with electrical activity. (**E**) Cross-correlation analysis revealed that the side without thalamic inputs was more synchronized.

in ACC, including changes in the duration, amplitude, onset location, and propagation velocity. Alterations in 2D CSD and spatiotemporal profiles after thalamic activity were desynchronized by thalamic afferents. Comparisons of the epileptiform activity obtained between cingulate cortices with and without thalamic inputs showed the following: (1) cortex lacking thalamic inputs were more susceptible to epileptiform activity, (2) duration of ACC seizure-like activities were enhanced without thalamic inputs and no significant difference in ACC seizure-like activities were observed between cortices with or without intact thalamic inputs when the concentration of bicuculline was 50 μM, (3) the onset of epileptiform activity shifted to layers V/VI (2D CSD profiles also revealed a pronounced sink signal after the thalamic inputs were removed), (4) calcium imaging demonstrated that calcium-mediated bursting was more synchronized in cortices with severed thalamic inputs. Therefore, thalamic inputs play a desynchronizing role in epileptiform activity and a mechanism of inhibition include thalamic driving of GABAergic interneurons that suppresses further augmentation of seizures.

The desynchronizing effect of thalamic inputs was involved in the suppression of seizures demonstrated by in vivo recording (Polack et al., 2009). TTX infusion into the ventroposterior medial thalamic nucleus in spontaneously epileptic rats to temporally suppress the activity of thalamic

relay neurons generated a longer duration SWD in somatosensory cortex. Our study using 4-AP and a low dose of bicuculline (5 μM) yielded similar results. This inhibitory effect on seizure-like activities might occur via activation of GABAergic transmission. Our results showed that bicuculline at 50 μM completely suppressed the GABAergic system and no significant difference was found between the intact thalamocortical (TC) and severed thalamic groups. Therefore, thalamic inputs may exert inhibitory effects via the GABAergic system in ACC.

Signal processing in the lateral propagation of electrical activity is under tight control, whereas unrestrained lateral propagation of electrical activity readily causes seizures. Epileptiform activity in neocortex is modulated by surrounding inhibition (Prince, 1967) and decreasing surrounding inhibition caused spreading of epileptiform activity (Pinto et al., 2005; Trevelyan et al., 2006). Research in hippocampal slices also showed that, when surrounding inhibition collapses, epileptiform activity becomes synchronized in different columns (Sloviter & Brisman, 1995). This phenomenon was demonstrated in our calcium imaging experiment where calcium transients tended to be more synchronized when the inhibitory effect of thalamic inputs was eliminated. Removing the thalamic inputs in our slice may have decreased the inputs that activate surrounding inhibition or desynchronized them, causing epileptiform activity to wane.

The onset location of epileptiform activity can arise from many different locations in ACC (Madhavan et al., 2007). When the thalamic inputs were intact, epileptiform activity was mostly initiated in layer II/III, and when thalamic inputs were removed, the onset sites shifted to layers V/VI. Previous studies suggested that impaired feed-forward inhibition from TC inputs might be the pathogenic cause of epilepsy in *tottering* transgenic mice (Sasaki et al., 2006). In our 2D CSD analysis, thalamic denervation produced more sink signals in the deep layers indicating that these layers are not subjected to thalamic inhibition. Thalamic inputs activate inhibitory interneurons and excitatory neurons, but interneurons respond more robustly to TC excitation (Contreras et al., 1997; Gibson et al., 1999; Bruno & Simons, 2002). In the normal physiologic condition, interneuron activation provides a time window for excitatory postsynaptic potentials elicited by TC activation in response to sensory stimuli (Miller et al., 2001; Douglas & Martin, 2004) and provides precise temporal resolution for sensory information processing. Inhibitory interneurons might also create a time window for the burst activity of pyramidal neurons. Therefore, when the thalamic inputs were intact, we found the initiation onset was in layer II/III, presumably where the thalamic inputs exert their modulatory function. The initiation regions of epileptiform activity moved to deeper layers after the thalamic inputs were removed, presumably because neurons in layer V have axons that project horizontally for several millimeters (Chagnac-Amitai et al., 1990; Williams & Stuart, 1999). This provided an anatomic basis for the synchronization of epileptogenic activity, which is initiated in layer V (Jones & Heinemann, 1988; Flint et al., 1997).

The cortex is sufficient for the switch of activity from normal to widespread synchronization of epileptiform activities. Previous studies also showed that infusion of bicuculline into the thalamus could generate 3 Hz neocortical discharges in rats (Castro-Alamancos, 1999). The variability of SWD initiation suggests that SWDs are generated by abnormal network oscillation, and can be initiated at several different parts within the network. In our studies, 4-AP/bicuculline-induced seizure-like activities are always began in the medial-ventral part of cortex in the MT-ACC slice.

Activity originated in area 24 propagated along the columnar organization. We found that the vertical velocity was faster than the horizontal propagation velocity showing that the lateral spreading of epileptiform activity is under the restraint of strong surrounding inhibition (Prince & Jacobs, 1998; Schwartz & Bonhoeffer, 2001).

Seizure onset might involve multiple limbic sites and some nuclei in thalamus such as the mediodorsal nucleus (Juhasz et al., 1999), centromedian nucleus (Velasco et al., 1995), and parafasicular nuclei (Langlois et al., 2010). These latter nuclei are involved in supporting limbic seizure propagation from a primary focus to other cortical and subcortical regions. These nuclei could play a pivotal role in the remote control of seizure activities and be an interesting target for deep brain stimulation (Kahane & Depaulis, 2010). The mediodorsal thalamic nucleus is thought to be involved in the modulation of seizures, specifically those involving limbic regions (Bertram et al., 1998, 2001). Previous clinical studies showed that electrical stimulation in MT can decrease seizure frequency (Sterman et al., 1982; Urino et al., 2010), and these results demonstrated that MT activities are involved in blocking seizures. Yet, the mechanisms by which thalamic stimulation through deep brain stimulation may reduce seizure frequency are not clear. Our results showed that the activity of thalamic inputs contributes to the desynchronization of seizure-like activities. In the present study, we used a 350 μA current with repeated 1 Hz stimulation of the MT and found reduced seizure-like activities, while stimulating the corpus callosum increased the occurrence of seizures. By comparing the efficiency of thalamic inputs and CC in the inhibition of epileptiform activity, we found that repeated stimulation of the thalamus efficiently inhibited epileptiform activity, demonstrating that the desynchronization was pathway-specific. The clinical implications of deep thalamic stimulation in the modulation of cingulate epileptic activity require further investigation.

Acknowledgments

We thank Dr. Chun-Kuei Su for helpful discussions. This study was supported by grants from the National Science Council (99-2320-B-001-016-MY3) and Academia Sinica, Taiwan.

Disclosure

None of the authors has any conflict of interest to disclose. We confirm that we have read the Journal's position on issues involved in ethical publication and affirm that this report is consistent with those guidelines.

References

Antognini JF, Carstens E, Sudo M, Sudo S. (2000) Isoflurane depresses electroencephalographic and medial thalamic responses to noxious stimulation via an indirect spinal action. *Anesth Analg* 91:1282–1288.

Avoli M, Barbarosie M, Lucke A, Nagao T, Lopantsev V, Kohling R. (1996) Synchronous GABA-mediated potentials and epileptiform discharges in the rat limbic system in vitro. *J Neurosci* 16:3912–3924.

Bancaud J, Talairach J. (1992) Clinical semiology of frontal lobe seizures. *Adv Neurol* 57:3–58.

Bertram EH, Zhang DX, Mangan P, Fountain N, Rempe D. (1998) Functional anatomy of limbic epilepsy: a proposal for central synchronization of a diffusely hyperexcitable network. *Epilepsy Res* 32:194–205.

Bertram EH, Mangan PS, Zhang D, Scott CA, Williamson JM. (2001) The midline thalamus: alterations and a potential role in limbic epilepsy. *Epilepsia* 42:967–978.

Bruckner C, Stenkamp K, Meierkord H, Heinemann U. (1999) Epileptiform discharges induced by combined application of bicuculline and 4-aminopyridine are resistant to standard anticonvulsants in slices of rats. *Neurosci Lett* 268:163–165.

Bruno RM, Simons DJ. (2002) Feedforward mechanisms of excitatory and inhibitory cortical receptive fields. *J Neurosci* 22:10966–10975.

Castro-Alamancos MA. (1999) Neocortical synchronized oscillations induced by thalamic disinhibition in vivo. *J Neurosci* 19:RC27.

Chagnac-Amitai Y, Luhmann HJ, Prince DA. (1990) Burst generating and regular spiking layer 5 pyramidal neurons of rat neocortex have different morphological features. *J Comp Neurol* 296:598–613.

Chauvel P, Trottier S, Vignal JP, Bancaud J. (1992) Somatomotor seizures of frontal lobe origin. *Adv Neurol* 57:185–232.

Contreras D, Llinas R. (2001) Voltage-sensitive dye imaging of neocortical spatiotemporal dynamics to afferent activation frequency. *J Neurosci* 21:9403–9413.

Contreras D, Destexhe A, Steriade M. (1997) Intracellular and computational characterization of the intracortical inhibitory control of synchronized thalamic inputs in vivo. *J Neurophysiol* 78:335–350.

Devinsky O, Morrell MJ, Vogt BA. (1995) Contributions of anterior cingulate cortex to behaviour. *Brain* 118:279–306.

Douglas RJ, Martin KA. (2004) Neuronal circuits of the neocortex. *Annu Rev Neurosci* 27:419–451.

Flint AC, Maisch US, Kriegstein AR. (1997) Postnatal development of low [Mg2 +] oscillations in neocortex. *J Neurophysiol* 78:1990–1996.

Geier S, Bancaud J, Talairach J, Bonis A, Szikla G, Enjelvin M. (1977) The seizures of frontal lobe epilepsy. A study of clinical manifestations. *Neurology* 27:951–958.

Gibson JR, Beierlein M, Connors BW. (1999) Two networks of electrically coupled inhibitory neurons in neocortex. *Nature* 402:75–79.

Glenn LL, Hada J, Roy JP, Deschenes M, Steriade M. (1982) Anterograde tracer and field potential analysis of the neocortical layer I projection from nucleus ventralis medialis of the thalamus in cat. *Neuroscience* 7:1861–1877.

Glover WE. (1982) The aminopyridines. *Gen Pharmacol* 13:259–285.

Hatanaka N, Tokuno H, Hamada I, Inase M, Ito Y, Imanishi M, Hasegawa N, Akazawa T, Nambu A, Takada M. (2003) Thalamocortical and intracortical connections of monkey cingulate motor areas. *J Comp Neurol* 462:121–138.

Ikegaya Y, Le Bon-Jego M, Yuste R. (2005) Large-scale imaging of cortical network activity with calcium indicators. *Neurosci Res* 52:132–138.

Jones RS, Heinemann U. (1988) Synaptic and intrinsic responses of medical entorhinal cortical cells in normal and magnesium-free medium in vitro. *J Neurophysiol* 59:1476–1496.

Juhasz C, Nagy F, Watson C, da Silva EA, Muzik O, Chugani DC, Shah J, Chugani HT. (1999) Glucose and [11C]flumazenil positron emission tomography abnormalities of thalamic nuclei in temporal lobe epilepsy. *Neurology* 53:2037–2045.

Kahane P, Depaulis A. (2010) Deep brain stimulation in epilepsy: what is next? *Curr Opin Neurol* 23:177–182.

Klueva J, Munsch T, Albrecht D, Pape HC. (2003) Synaptic and non-synaptic mechanisms of amygdala recruitment into temporolimbic epileptiform activities. *Eur J Neurosci* 18:2779–2791.

Langlois M, Polack PO, Bernard H, David O, Charpier S, Depaulis A, Deransart C. (2010) Involvement of the thalamic parafascicular nucleus in mesial temporal lobe epilepsy. *J Neurosci* 30:16523–16535.

Lee CM, Chang WC, Chang KB, Shyu BC. (2007) Synaptic organization and input-specific short-term plasticity in anterior cingulate cortical neurons with intact thalamic inputs. *Eur J Neurosci* 25:2847–2861.

Lundh H, Nilsson O, Rosen I. (1984) Treatment of Lambert-Eaton syndrome: 3,4-diaminopyridine and pyridostigmine. *Neurology* 34:1324–1330.

Madhavan D, Liebman T, Nadkarni S, Devinsky O. (2007) Anterior cingulate epilepsy in an 18-year-old woman. *Rev Neurol Dis* 4:39–42.

Mazars G. (1970) Criteria for identifying cingulate epilepsies. *Epilepsia* 11:41–47.

McCagh J, Fisk JE, Baker GA. (2009) Epilepsy, psychosocial and cognitive functioning. *Epilepsy Res* 86:1–14.

Miller KD, Pinto DJ, Simons DJ. (2001) Processing in layer 4 of the neocortical circuit: new insights from visual and somatosensory cortex. *Curr Opin Neurobiol* 11:488–497.

Nadkarni S, Devinsky O. (2009) *Cingulate cortex seizures*. Oxford University Press, New York.

Panuccio G, Curia G, Colosimo A, Cruccu G, Avoli M. (2009) Epileptiform synchronization in the cingulate cortex. *Epilepsia* 50:521–536.

Pinto DJ, Patrick SL, Huang WC, Connors BW. (2005) Initiation, propagation, and termination of epileptiform activity in rodent neocortex in vitro involve distinct mechanisms. *J Neurosci* 25:8131–8140.

Polack PO, Mahon S, Chavez M, Charpier S. (2009) Inactivation of the somatosensory cortex prevents paroxysmal oscillations in cortical and related thalamic neurons in a genetic model of absence epilepsy. *Cereb Cortex* 19:2078–2091.

Prince DA. (1967) Electrophysiology of ''epileptic neurons''. *Electroencephalogr Clin Neurophysiol* 23:83–84.

Prince DA, Jacobs K. (1998) Inhibitory function in two models of chronic epileptogenesis. *Epilepsy Res* 32:83–92.

Rasmussen T. (1983) Characteristics of a pure culture of frontal lobe epilepsy. *Epilepsia* 24:482–493.

Sasaki S, Huda K, Inoue T, Miyata M, Imoto K. (2006) Impaired feedforward inhibition of the thalamocortical projection in epileptic Ca2 + channel mutant mice, tottering. *J Neurosci* 26:3056–3065.

Schwartz TH, Bonhoeffer T. (2001) In vivo optical mapping of epileptic foci and surround inhibition in ferret cerebral cortex. *Nat Med* 7:1063–1067.

Shimono K, Taketani M, Brucher F, Kubota D, Colgin L, Robertson S. (2001) Continuous two-dimensional current source density analyses of electrophysiological. *Neurocomputing* 38–40:899–905.

Shulman MB. (2000) The frontal lobes, epilepsy, and behavior. *Epilepsy Behav* 1:384–395.

Sloviter RS, Brisman JL. (1995) Lateral inhibition and granule cell synchrony in the rat hippocampal dentate gyrus. *J Neurosci* 15:811–820.

Sterman MB, Shouse MN, Passouant P. (1982) *Sleep and epilepsy*. Academic Press, New York.

Traub RD, Contreras D, Cunningham MO, Murray H, LeBeau FE, Roopun A, Bibbig A, Wilent WB, Higley MJ, Whittington MA. (2005) Single-column thalamocortical network model exhibiting gamma oscillations, sleep spindles, and epileptogenic bursts. *J Neurophysiol* 93:2194–2232.

Trevelyan AJ, Sussillo D, Watson BO, Yuste R. (2006) Modular propagation of epileptiform activity: evidence for an inhibitory veto in neocortex. *J Neurosci* 26:12447–12455.

Urino T, Hashizume K, Maehara M, Kato K, Okada Y, Hori T, Tanaka T. (2010) Epileptic focus stimulation and seizure control in the rat model of kainic acid-induced limbic seizures. *Neurol Med Chir (Tokyo)* 50:355–360.

Velasco F, Velasco M, Velasco AL, Jimenez F, Marquez I, Rise M. (1995) Electrical stimulation of the centromedian thalamic nucleus in control of seizures: long-term studies. *Epilepsia* 36:63–71.

Vogt BA. (2005) Pain and emotion interactions in subregions of the cingulate gyrus. *Nat Rev Neurosci* 6:533–544.

Vogt BA, Pandya DN, Rosene DL. (1987) Cingulate cortex of the rhesus monkey: I. Cytoarchitecture and thalamic afferents. *J Comp Neurol* 262:256–270.

Williams SR, Stuart GJ. (1999) Mechanisms and consequences of action potential burst firing in rat neocortical pyramidal neurons. *J Physiol* 521:467–482.

Supporting Information

Additional Supporting Information may be found in the online version of this article:

Figure S1. Pyramidal neurons generate inhibitory currents and decrease firing.

Figure S2. Local application of lidocaine to MT enhances seizure-like activities in the ACC.

Figure S3. Thalamic inputs modulate the velocity of epileptiform activity.

Please note: Wiley-Blackwell is not responsible for the content or functionality of any supporting information supplied by the authors. Any queries (other than missing material) should be directed to the corresponding author for the article.